


Article

MoS₂ QDs/8-Armed Poly(Ethylene Glycol) Fluorescence Sensor for Three Nitrotoluenes (TNT) Detection

Xiaoyuan Zhang and Zhiqiang Su * 

State Key Laboratory of Chemical Resource Engineering, Beijing Key Laboratory of Advanced Functional Polymer Composites, Beijing University of Chemical Technology, Beijing 100029, China; 2020700036@buct.edu.cn

* Correspondence: suzq@mail.buct.edu.cn

Abstract: In this work, ammonia cross-linked 8-armed polyethylene glycol hydrogel material was successfully synthesized and used as a template for synthesizing nanoparticles with fluorescent properties. The 8-armed polyethylene glycol hydrogel template was used to prepare molybdenum disulfide quantum dots (MoS₂ QDs). The ammonium tetrathiomolybdate functioned as a molybdenum source and hydrazine hydrate functioned as a reducing agent. The fluorescence properties of the as-prepared MoS₂ QDs were investigated. The bursting of fluorescence caused by adding different concentrations of explosive TNT was studied. The study indicated that the synthesized MoS₂ QDs can be used for trace TNT detection with a detection limit of 6 nmol/L and a detection range of 16–700 nmol/L. Furthermore, it indicated that the fluorescence-bursting mechanism is static bursting.

Keywords: hydrogel; fluorescent sensor; TNT detection; molybdenum disulfide; bionanomaterials



Citation: Zhang, X.; Su, Z. MoS₂ QDs/8-Armed Poly(Ethylene Glycol) Fluorescence Sensor for Three Nitrotoluenes (TNT) Detection. *Biosensors* **2021**, *11*, 475. <https://doi.org/10.3390/bios11120475>

Received: 27 October 2021

Accepted: 23 November 2021

Published: 25 November 2021

Publisher's Note: MDPI stays neutral with regard to jurisdictional claims in published maps and institutional affiliations.



Copyright: © 2021 by the authors. Licensee MDPI, Basel, Switzerland. This article is an open access article distributed under the terms and conditions of the Creative Commons Attribution (CC BY) license (<https://creativecommons.org/licenses/by/4.0/>).

1. Introduction

Hydrogel is a polymer with a cross-linked three-dimensional network structure with hydrophilic groups. It can swell in water but is insoluble in water [1], and is an essential functional polymer material. Hydrogels contain hydrophilic groups that can absorb large quantities of water, which causes them to swell. Most hydrogels have a high water content, low modulus, and solid shape [2]. The multi-arm polyethylene glycol hydrogel material is a new type of polyethylene glycol hydrogel. It has various advantages that long-chain hydrogels do not have: high mechanical strength, high toughness, easy to prepare, and biocompatibility.

In recent years, molybdenum disulfide (MoS₂) research has focused on the application of electrical and catalytic properties, and the related optical applications have not been widely studied. Since its discovery in 2004, single-atom-thick graphene has been widely used in interdisciplinary fields. Graphene materials have caused a sensation in physics, chemistry, materials science, nanoscience, engineering, and biology [3–6]. The excellent physical and chemical properties of graphene depend primarily on its inherent two-dimensional properties [7]. Many ultra-thin nanosheets of graphene-like two-dimensional inorganic materials such as MoS₂ and tungsten disulfide are often used for cutting-edge research [8–10]. MoS₂ has attracted particular attention because it can be easily peeled off. Moreover, MoS₂ is a material with a specific energy bandgap and has high chemical and thermal stability. Its properties increase the difficulty of preparing fluorescent molybdenum disulfide materials. Therefore, it is imperative to study the synthesis method of MoS₂ materials with a fluorescent effect.

Some fluorescent MoS₂ materials are beginning to be fabricated. In 2010, Splendiani et al. manufactured MoS₂ material on quartz and Si/SiO₂ wafers using micro-lifting technology and reported the fluorescent application of this material for the first time [11]. In 2011, Coleman et al. prepared fluorescent MoS₂ utilizing ultrasonic waves in a suitable organic solvent, which is a commercialized efficient MoS₂ stripping method [12]. Eda

et al. prepared MoS₂ with a fluorescence effect through ultrasonic treatment and Li intercalation [13]. Stengl et al. prepared MoS₂ QDs using ultrasonic treatment and liquid phase exfoliation [14]. Lin et al. prepared MoS₂ QDs with different functionalizations through surface modification of MoS₂ QDs with thiol-containing capping agents using a simple hydrothermal method [15]. Wu et al. [16] synthesized cysteine-functionalized MoS₂ quantum dots (Cys-MoS₂ QDs) by a simple amidation reaction, finding that Cys-MoS₂ QDs had stable fluorescence. Roy et al. [17] synthesized water-soluble MoS₂ QDs using a simplistic bottom-up hydrothermal method.

Similarly, chemical vapor deposition methods are used to synthesize MoS₂ films with fluorescence effects on various substrates [18], and MoS₂ films are prepared by Ar⁺ plasma irradiation methods [19]. Most of the preparation methods for MoS₂ QDs are “top-down” preparation methods. These methods usually have many shortcomings, such as environmental sensitivity, massive energy consumption, the use of expensive and harmful organic solvents, and harsh pretreatment. “Bottom-up” methods such as hydrothermal synthesis have also been reported to synthesize fluorescent MoS₂ QDs [20]. However, hydrothermal synthesis methods also have some shortcomings. For example, the synthesized products need to be separated for a long time. The reaction temperature is relatively high, and a high-pressure vessel is required. These problems may be able to be solved by using the template method, but not many studies investigate this method.

2,4,6-Trinitrotoluene (TNT) is an important nitroaromatic explosive [21], which has explosive solid power. Because of its use in terrorist activities, a quick and straightforward technical means to detect TNT is needed. Moreover, TNT is considered a substance harmful to the environment that has a lasting adverse effect on the health of humans and wild animals [22]. Therefore, in the following work, a fluorescence sensor is designed to detect TNT with the fluorescence quenching effect based on MoS₂ QDs. This work uses 8-arm polyethylene glycol hydrogel as a template material to synthesize QDs materials. Using acrylate-terminated polyethylene glycol (PEGOA) as a template, there is no need for expensive reagents, hydrothermal conditions, other mechanical equipment, and complicated post-processing procedures. The PEGOA is cross-linked by ammonia at room temperature, reduced by hydrazine hydrate, and degraded. MoS₂ QDs with fluorescence effect will be prepared. 2,4,6-Trinitrotoluene (TNT) was selected as the target analyte. Studying the TNT concentration and the fluorescence emission intensity data of MoS₂ QDs will provide the possible fluorescence quenching mechanism.

2. Materials and Methods

2.1. Materials

8-armed polyethylene glycol (8PEG-OH, Mw 15 kDa) was purchased from Jenkem Technologies, Plano, TX, USA. 8-armed polyethylene glycol acrylate (8PEG) was prepared using the same procedure as previously reported [23]. Polyethylene glycol diacrylate (PEGDA, Mw = 2 kDa), ammonium tetrathiomolybdate (98% purity), and TNT (1 mg/L ethanol standard solution) were purchased from Beringer (St. Helena, CA, USA). Ammonia (37% w/w) and hydrazine hydrate were purchased from the China Pharmaceutical Group (Shanghai, China). All other reagents were purchased from Aldrich and used as is unless otherwise stated. Solvents were of at least analytical quality.

2.2. Synthesis of Acryloyl Chloride Modified 8-Armed Polyethylene Glycol (PEGOA)

First, 8PEG-OH (5 g) with hydroxyl capping was synthesized in a dry vacuum oven at 60 °C. 8PEG-OH was dissolved in 50 mL of Superdry solvent under nitrogen, and then the solution was placed in an ice-water bath. Then, 4 g of sodium carbonate was added to this mixture to neutralize the esterification reaction and produce the acid. The solution was stirred and reacted with a magnetic stirrer at 35 °C for 4 days under a continuous stream of nitrogen. The reacted solution was filtered through a column of alkaline alumina to remove the insoluble solids and the acid produced during the reaction. The solution was evaporated under a vacuum at 20 °C until a specific concentration was reached. An excess

of cooled anhydrous ether ($<4\text{ }^{\circ}\text{C}$) was added dropwise to the solution. The concentrated solution was collected in a centrifuge tube, stirred continuously, and centrifuged rapidly (5000 rpm, 15 min). After centrifugation was allowed to settle, the lower sediment was taken and dried in a vacuum oven at $40\text{ }^{\circ}\text{C}$ for 6 h to obtain a white powdery solid. The dried final product was weighed, and the yield was calculated. The yield was about 72%.

2.3. Preparation of Ammonium Tetrathiomolybdate Solution

100 mg of ammonium tetrathiomolybdate was dissolved in 1 mL of ultrapure water to obtain an ammonium tetrathiomolybdate solution with a 0.1 mg/mL concentration. The ammonium tetrathiomolybdate decomposed easily in an aqueous solution and was easy to prepare.

2.4. Synthesis of MoS_2 QDs by 8-Armed Polyethylene Glycol Hydrogel Template Method

Three pre-prepared portions of 150 mg PEGOA were placed in 5 mL plastic centrifuge tubes. Then, 150 mL of ultrapure water was added to dissolve them. For half an hour, an ultrasonic cleaner was used for ultrasonic treatment to ensure that the solution was completely dissolved and free of inclusions or bubbles. After ultrasonic treatment, 20 μL of ammonium tetrathiomolybdate solution was added to the PEGOA solution. After evenly mixing ammonium tetrathiomolybdate and PEGOA solution, 30 μL of ammonia, 30 μL of a mixture of ammonia and hydrazine hydrate with a mass ratio of 1:1, and 30 μL of hydrazine hydrate were added to the PEGOA and ammonium tetrathiomolybdate solution. The three mixed solutions were then rapidly shaken and placed in an ultrasonic cleaner for 15 min to form the gum. 2 mL of ultrapure water was added to all three kinds of solutions and set at room temperature for four days for gel formation.

2.5. Instruments and Measurements

2.5.1. UV-Vis Spectroscopic Testing

2 mL of the newly synthesized products of MoS_2 QDs were added to ammonia water, ammonia and hydrazine hydrate, and hydrazine hydrate only. At the same time, 2 mL of the mixture solution of ammonium tetrathiomolybdate and 8-arm polyethylene glycol with the same concentration were added. The four solutions were diluted to about 10 mg/L with MiliQ water and put into quartz test tubes. The UV absorption spectrum was recorded at room temperature with a TU-1901 UV-Vis spectrophotometer. The test range was 200–400 nm, the scanning rate was 100 nm/min, and the aqueous solution was the reference solution.

2.5.2. Dynamic Light Scattering (DLS) Testing

The four solutions were diluted to about 2.0×10^{-5} mol/L with miliQ water. The particle size and distribution of the solution were analyzed by a BI-90 plus dynamic light scattering particle sizer. The particle size and its distribution were calculated with the Stokes-Einstein equation.

2.5.3. X-ray Photoelectron Spectroscopy (XPS)

A total of 2 mL of the four solutions were refrigerated at $-4\text{ }^{\circ}\text{C}$. They were then freeze-dried at $-60\text{ }^{\circ}\text{C}$, 20 Pa, for 3 days. After the freeze-drying process was complete, the obtained powder was evenly applied to the conductive adhesive. The X-ray source was al $\text{K}\alpha$ Ray (1486.6 eV), and the beam spot size was 400 μm . The energy of full-spectrum scanning was 150 eV, and the step size was 1 eV. The ESCALAB 250 photoelectron spectrometer was utilized for the test. The test results were plotted and analyzed using Origin 8.5 software.

2.5.4. Fluorescence Emission Spectra

At room temperature, the excitation wavelengths of four solutions were scanned with a LS-55 fluorescence spectrometer (PerkinElmer, Inc., Boston, MA, USA). The test

conditions were set a slit width of 5 nm and scanning rate of 100 nm/min. We started scanning at a fixed excitation wavelength of 320 nm and calculated the Stokes displacement. Then, we gradually changed the excitation wavelength from 280 nm and obtained the corresponding emission wavelength.

2.5.5. High-Resolution Transmission Electron Microscopy (HR-TEM) Measurement

The aqueous solution of PEGOA hydrogel degradation products containing MoS₂ QDs was diluted slightly. A small amount of the solution was dropped onto the copper mesh loaded with ultra-thin carbon film with a pipette gun. The samples were allowed to air-dry overnight at room temperature. The samples were observed with a JEM-3030F high-transmission electron microscope at different magnifications. The acceleration voltage was 200 kV. There was minor damage to the material surface under this condition.

2.5.6. Fluorescence Detection of TNT

The degradation products of PEGOA hydrogel MoS₂ QDs with ammonia and hydrazine hydrate were extracted at 2 mL and diluted below the maximum detection limit of the LS-55 fluorescence spectrometer. The fluorescence spectrum test conditions in previous studies were the same. TNT solutions with different concentrations were prepared. The TNT solutions were added to the solution containing degradation products of MoS₂ QDs with a pipette gun. The concentration of TNT solution was changed from 0 to 1000 nmol/L. The excitation wavelength of fixed fluorescence was 340 nm. The change of fluorescence intensity was measured at the emission wavelength of 416 nm. The slit width was 5 nm, and the scanning rate was 100 nm/min.

3. Results and Discussion

3.1. MoS₂ QDs Fabrication with the PEGOA Template Method

MoS₂ QDs were prepared with the PEGOA template method, which is different from the MoS₂ QDs synthesized in existing techniques. MoS₂ QDs products were designed with PEGOA as the template and ammonium tetrathiomolybdate as the molybdenum source. The product obtained by crosslinking PEGOA with ammonia was a light yellow solution without precipitation. It took a long time to reduce ammonium tetrathiomolybdate to synthesize QDs. A group of products added to PEGOA and hydrazine hydrate were dark brown solutions and suspended brown particles. This showed that the volume-limiting effect is not strong when only in the presence of PEG molecular chains. However, its reducibility is strong, and it produces the MoS₂ particle with an indefinite diameter. Most of the control groups without PEGOA produced black residues, indicating that ammonium tetrathiomolybdate can only be reduced to MoS₂ precipitate insoluble in water without polymer chains. The product had no practical value. Unlike the product without the PEGOA template, the MoS₂ QDs synthesized by the PEGOA hydrogel template were transparent solutions without residues and insoluble substances, and did not need any separation treatment. This indicates that the PEGOA hydrogel template method is a fast and straightforward method for preparing MoS₂ QDs.

The formation of MoS₂ QDs is schematically drawn in Figure 1a. Figure 1b,c shows that the particle size of the MoS₂ QDs was relatively large, as observed by HR-TEM. In our previous work, the 8PEG hydrogel was used as a template to synthesize AgNCs. [24] The formation was due to the volume-limiting effect of 8PEG networks to AgNCs. The AgNCs formed inside the nanocages of the formed 8PEG gels. Results showed a homogenous distribution of AgNCs in the gel matrix. This previous work inspired us with the idea to attempt MoS₂ QDs in situ formation. This is because the quantum dots displayed partial agglomeration, as well as because the core-shell structure of the synthesized QDs was caused by polyethylene glycol degradation. The existence of a single nanoparticle can still be seen from the electron micrograph with a larger magnification. Its particle size is about 10 nm, indicating that molybdenum disulfide grows within the pore size of the PEGOA gel. The formation of MoS₂ QDs is limited in 8PEG networks, resulting in imperfect layered

morphologies of MoS₂ QDs. In addition, the formed MoS₂ QDs are similar to nanoparticles. They are different from the layered 2D MoS₂ QDs.

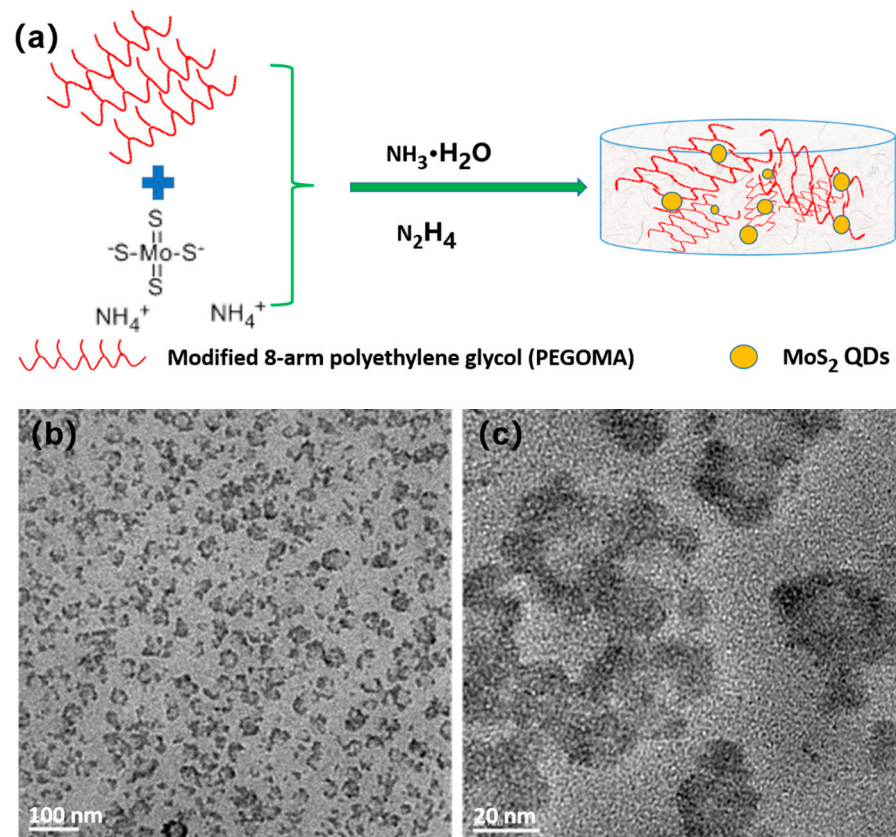


Figure 1. (a) Schematic drawing of MoS₂ QDs formation; HR-TEM (b) image and (c) magnified image of MoS₂ QDs synthesized by the template.

The X-ray photoelectron spectroscopy (XPS) analysis of MoS₂ products synthesized by the PEGOA hydrogel template method is shown in Figure 2. XPS data show that the sample contains sulfur, nitrogen, oxygen, carbon, hydrogen, and molybdenum. The presence of nitrogen indicates that ammonia successfully acts as a crosslinking agent. The sulfur element in MoS₂ QDs prepared by the PEGOA hydrogel template method has a weak peak at 162.2 eV. The Mo3d peaks have orbital self-selected split peaks, Mo3d_{5/2} and Mo3d_{3/2}, positioned around 230 eV and 234 eV in the figure, respectively. This is the characteristic peak of MoS₂, indicating that PEGOA can be used as a template for preparing MoS₂ QDs.

3.2. Photoluminescence Performance Analysis of MoS₂ QDs

8-armed star-shaped PEG-based hydrogels (8PEG-NH₃) can be cross-linked by ammonium solution [19]. These were formed by an amine Michael-type addition reaction between unsaturated carbon-carbon double bonds (acrylate end groups) and reactive amine species. The degree of residual functional groups, the swelling degree, and the resulting gels' mechanical properties can be tuned [25,26].

Figure 3 shows the UV spectra of the MoS₂ QDs synthesized by the above methods. The UV spectrum of the ammonia water group has a specific UV absorption near 285 nm. The UV absorption peak at 285 nm only appeared in the ammonia group. This is because the added ammonium tetrathiomolybdate could not be reduced entirely. The intermediate product may have a certain degree of UV absorption near 285 nm.

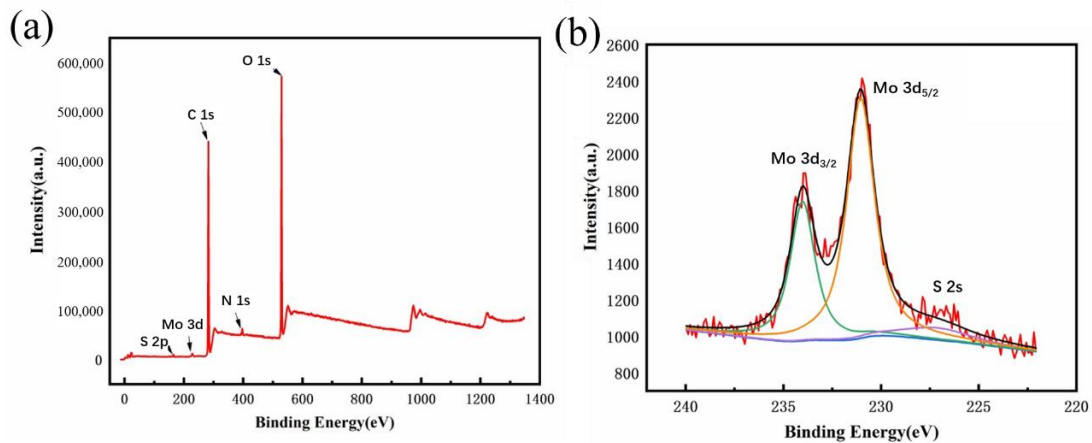


Figure 2. The X-ray photoelectron spectroscopy (XPS) (a) survey analysis and (b) Mo3d of MoS₂ products.

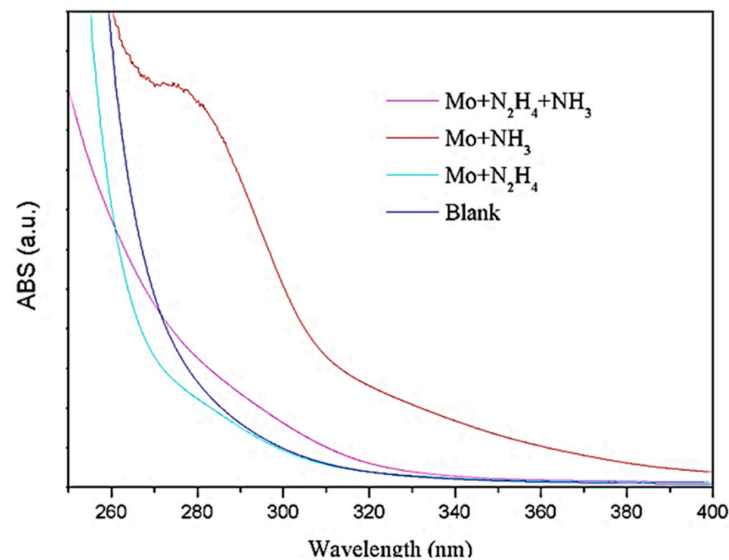


Figure 3. UV-Vis spectrogram of synthesized MoS₂ QDs by the above methods.

Figure 4 shows the dynamic light scattering (DLS) analysis of MoS₂ QDs prepared with the PEGOA template using NH₃, NH₃ + N₂H₄, and N₂H₄ cross-linking agents, respectively. It can be seen from the figure that the particle size of ammonia as the additive is typically around 4.8 nm. The size of the mixture of ammonia and hydrazine hydrate is mostly about 4.1 nm. The size of hydrazine hydrate as the additive is mostly about 615 nm. This phenomenon further indicates the formation of MoS₂ QDs in the PEGOA template.

Figure 5 shows the excitation spectra obtained by scanning the MoS₂ QDs when the fluorescence emission spectrum was set to 420 nm. All solutions are filtered and removed through a tetrafluoroethylene filter so as not to damage the instrument while measuring the insoluble. The blank control group without PEGOA has a weak excitation peak at 365 nm, which may be the excitation peak of solvent water. The excitation peak of the MoS₂ QDs product obtained by adding only hydrazine hydrate is shallow and wide. This indicates that the particle size distribution of MoS₂ QDs obtained by reducing only hydrazine hydrate is wide. The width of the excitation peaks when only ammonia is added is much lower than that when only hydrazine hydrate is added. There are two little peaks at 330 nm and 360 nm, indicating that the reduction reaction occurs very slowly and only partially. The possible reason is that MoS₂ QDs are synthesized inside the PEGOA hydrogel, and some may be synthesized outside the hydrogel, resulting in uneven particle size distribution. The ammonia and hydrazine hydrate groups show a strong excitation

peak near 340 nm. The peak width was narrow, indicating that QDs with uniform particle size were synthesized inside the hydrogel.

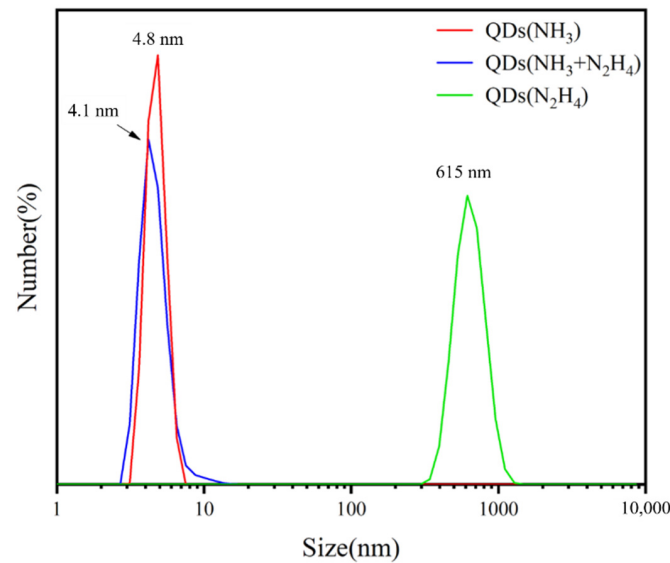


Figure 4. Dynamic light scattering (DLS) analysis of MoS₂ QDs.

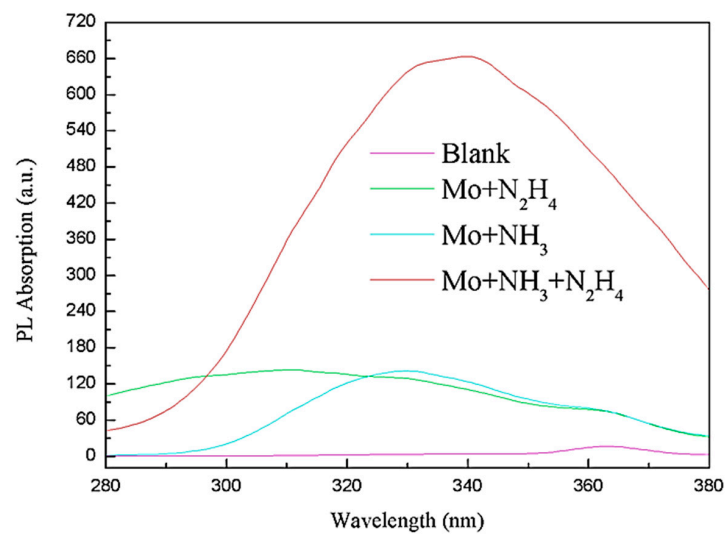


Figure 5. Fluorescence excitation spectrum of MoS₂ QDs synthesized by above methods when emission spectrum is set as 420 nm.

Since the MoS₂ QDs have the most substantial excitation peak at 340 nm, we set the excitation light wavelength to 340 nm to detect the fluorescence emission spectra of the four groups of MoS₂ products. The results are shown in Figure 6. The product obtained without PEGOA in the control group has a weak emission peak near 414 nm, which may be a trace amount of MoS₂ QDs mixed with impurities. The group with only ammonia water and the group with only hydrazine hydrate showed multi-peak distribution. The peak positions ranged from 350 to 416 nm, indicating that the product's particle size obtained without volume limitation fully reduced was unevenly distributed. The fluorescence emission peak position obtained by adding ammonia and hydrazine hydrate is at 416 nm, consistent with the results described in other documents. This is the fluorescence emission peak of MoS₂ QDs. The peak width is narrow, indicating that particle size distribution of QD formation is relatively uniform. The Stokes shift of the obtained QDs is 76 nm, which may be one of the characteristics of QDs synthesized by the template method.

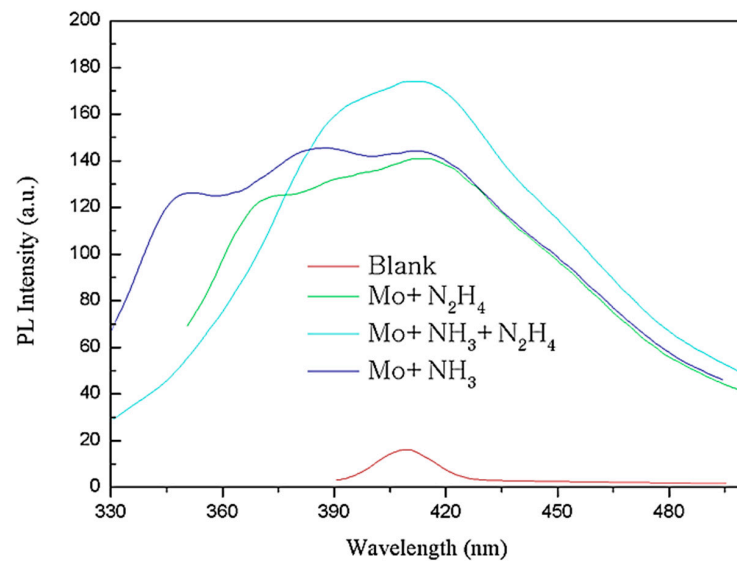


Figure 6. Fluorescence emission spectrum of MoS₂ QDs synthesized by the above methods when excitation spectrum is set as 340 nm.

Studying the position and intensity change of the emission peak of the MoS₂ QDs can better explain the difference in the particle sizes of the synthesized QDs. As shown in Figure 7, when the excitation wavelength is increased from 285 nm to 345 nm, the peak position of the emission spectrum changes between 416–421 nm. Moreover, the peak position of the emission spectrum changes only 5 nm when the excitation wavelength changes by 60 nm. This further illustrates the advantages of the template method, which are particle size control and narrow distribution. When the peak is more significant than 345 nm, the emission spectrum drops quickly, indicating that the fluorescence excitation peak of the prepared QDs is at 340 nm. It can be seen that a slight red shift of the fluorescence emission appears with the excitation wavelength. The redshift or change in the maximum intensity indicates a change in fluorescence properties, resulting from an interaction between the 8PEG and MoS₂ QDs. It is suggested that the change in fluorescence is due to the further growth of MoS₂ QDs.

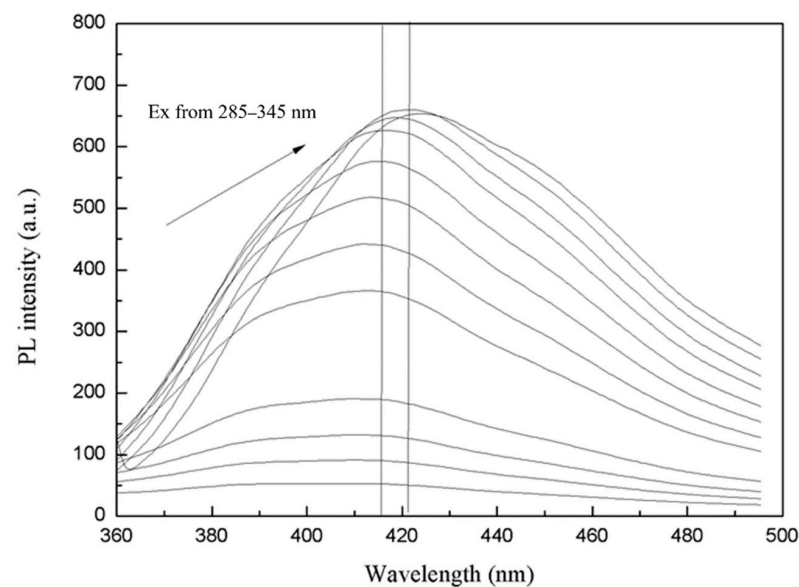


Figure 7. Emission spectrum of MoS₂ QDs changes along with excitation spectrum.

3.3. MoS₂ QDs for Fluorescence Detection of TNT

In Figure 8a, when a certain amount of TNT solution is added to the aqueous solution of MoS₂ QDs, the fluorescence emitted by the MoS₂ QDs is absorbed by the TNT molecules. This phenomenon can be attributed to fluorescence resonance energy transfer, resulting in the fluorescence quenching effect. The detection limit of the MoS₂ QDs prepared by the template method is 8 nmol/L. This value is determined by adding a certain amount of TNT solution, and the fluorescence quenching intensity is more significant than the three standard deviations detected by the instrument [27].

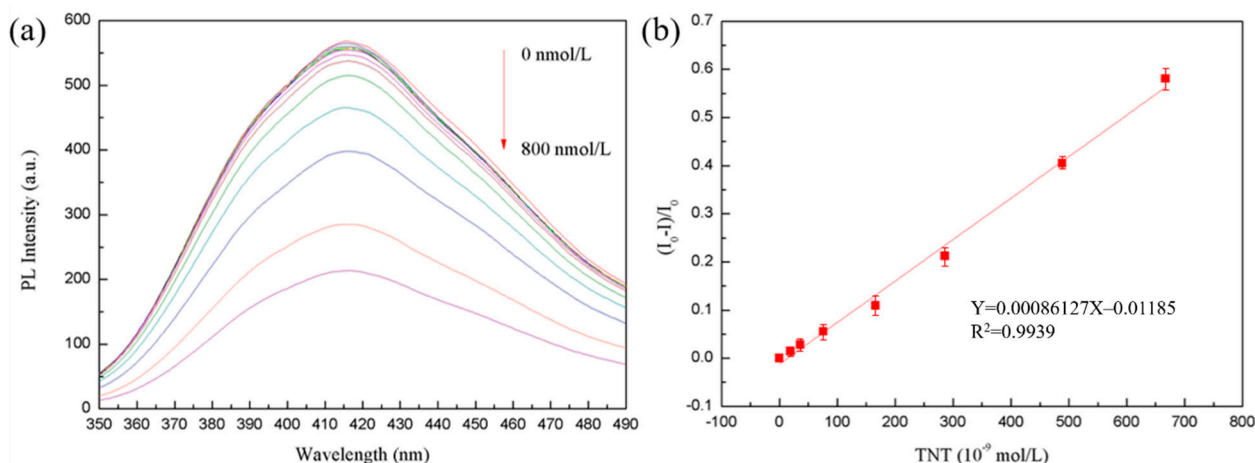


Figure 8. (a) Intensity of emission spectrum of MoS₂ QDs change with TNT concentration. (b) Detection range of MoS₂ QDs synthesized by the PEGOA template.

Figure 8b showed the fluorescence quenching degree (the ratio of fluorescence intensity after adding TNT to solution without quencher) of MoS₂ QDs. The fluorescence intensity is used as a characterization of the degree of fluorescence quenching. It can be seen that the fluorescence quenching degree $(I_0 - I)/I_0$ has a linear relationship with the concentration of TNT solution. In the range of TNT concentration of 16–700 nmol/L, the linear correlation coefficient is 0.9939, and the linear equation is $Y = 0.00086127X - 0.01185$. This indicates that MoS₂ QDs can be used as a fluorescence detection method to detect TNT in the linear range. The detection range is 16–700 nmol/L.

The quenching mechanism of TNT can be determined according to the following Lineweaver-Burk equation:

$$1/(F_0 - F) = 1/F_0 + K_{LB}/(F_0 C_q) \quad (1)$$

where F_0 and F are the fluorescence intensity of QDs when TNT is not added and when TNT is added, respectively. K_{LB} is the corresponding static quenching constant, and C_q is the concentration of the quencher. It can be seen from the formula that if $(F_0 - F)/F_0$ is proportional to the concentration of the liquid, the mechanism of fluorescence quenching is static quenching. Compared with the research of Xu et al., the detection limit of the sensor in this paper is reduced, which is of great significance to the improvement of the detection sensitivity of TNT [28,29]. In this work, the mechanism of sudden extinction is the coordination structure formed between MoS₂ QDs and TNT molecules. The TNT molecules absorb the fluorescence emission of MoS₂ QDs, which results in fluorescence quenching.

4. Conclusions

In summary, a novel ammonia cross-linked acrylate-terminated polyethylene glycol (PEGOA) hydrogel template was synthesized and used to prepare the nanocrystalline material MoS₂ QDs. MoS₂ QDs prepared by the template method have a controllable

particle size, narrow distribution, and stable fluorescence. They were influenced by the different components of the incorporated cross-linking and reducing agents. The burst effect of adding different concentrations of explosive TNT to the synthesized quantum dots on the fluorescence was investigated. This investigation indicated that the synthesized MoS₂ QDs can be used for trace TNT detection with a detection limit of 6 nmol/L and a detection range of 16–700 nmol/L. In the future, the quantum dots prepared by the template method could be used in the fields of catalytic synthesis, cellular fluorescence tracing, and fluorescence detection.

Author Contributions: X.Z. accomplished the manuscript; Z.S. proposed this project and supervised the experiments. All authors have read and agreed to the published version of the manuscript.

Funding: The authors greatly acknowledge the National Natural Science Foundation of China (NSFC, Grant No. 51873016), the Joint Project of BRC-BC (Biomedical Translational Engineering Research Center of BUCT-CJFH) (XK2020-11) and the Fundamental Research Funds for the Central Universities (ZY2103) for financial support.

Institutional Review Board Statement: Not applicable.

Informed Consent Statement: Not applicable.

Data Availability Statement: Not applicable.

Acknowledgments: Z.S. acknowledges the financial supports from the National Natural Science Foundation of China (NSFC, Grant no. 51873016) and the Joint Project of BRC-BC (Biomedical Translational Engineering Research Center of BUCT-CJFH) (XK2020-11). X.Z. acknowledges the Fundamental Research Funds for the Central Universities (ZY2103).

Conflicts of Interest: The authors declare no conflict of interest.

References

1. Kopeček, J. Hydrogel Biomaterials: A Smart Future? *Biomaterials* **2007**, *34*, 5185–5192. [[CrossRef](#)] [[PubMed](#)]
2. Takuro, M.; Sakai, T.; Akagi, Y.; Chung, U.; Shibayama, M. Sans and SIs Studies on Tetra-Arm Peg Gels in as-Prepared and Swollen States. *Macromolecules* **2009**, *16*, 6245–6252.
3. Novoselov, K.S.; McCann, E.; Morozov, S.V.; Fal'ko, V.I.; Katsnelson, M.I.; Zeitler, U.; Jiang, D.; Schedin, F.; Geim, A.K. Unconventional Quantum Hall Effect and Berry's Phase of 2π in Bilayer Graphene. *Nat. Phys.* **2006**, *2*, 177–180. [[CrossRef](#)]
4. Terrones, M.; Botello-Méndez, A.R.; Campos-Delgado, J.; López-Urías, F.; Vega-Cantú, Y.I.; Rodríguez-Macías, F.J.; Elías, A.L.; Muñoz-Sandoval, E.; Cano-Márquez, A.G.; Charlier, J.C.; et al. Graphene and Graphite Nanoribbons: Morphology, Properties, Synthesis, Defects and Applications. *Nano Today* **2010**, *4*, 351–372. [[CrossRef](#)]
5. Yu, X.; Zhang, W.; Zhang, P.; Su, Z. Fabrication Technologies and Sensing Applications of Graphene-Based Composite Films: Advances and Challenges. *Biosens. Bioelectron.* **2017**, *89*, 72–84. [[CrossRef](#)] [[PubMed](#)]
6. Li, Y.; Zhang, W.; Zhang, L.; Li, J.; Su, Z.; Wei, G. Sequence-Designed Peptide Nanofibers Bridged Conjugation of Graphene Quantum Dots with Graphene Oxide for High Performance Electrochemical Hydrogen Peroxide Biosensor. *Adv. Mater. Interfaces* **2017**, *3*, 1600895. [[CrossRef](#)]
7. Li, D.; Zhang, W.; Yu, X.; Wang, Z.; Su, Z.; Wei, G. When Biomolecules Meet Graphene: From Molecular Level Interactions to Material Design and Applications. *Nanoscale* **2016**, *47*, 19491–19509. [[CrossRef](#)]
8. Tzalenchuk, A.; Lara-Avila, S.; Kalaboukhov, A.; Paolillo, S.; Syväjärvi, M.; Yakimova, R.; Kazakova, O.; Janssen, T.J.; Fal'ko, V.; Kubatkin, S. Towards a Quantum Resistance Standard Based on Epitaxial Graphene. *Nat. Nanotechnol.* **2010**, *3*, 186–189. [[CrossRef](#)]
9. Gutiérrez, H.R.; Perea-López, N.; Elías, A.L.; Berkdemir, A.; Wang, B.; Lv, R.; López-Urías, F.; Crespi, V.H.; Terrones, H.; Terrones, M. Extraordinary Room-Temperature Photoluminescence in Triangular WS₂ Monolayers. *Nano Lett.* **2013**, *8*, 3447–3454. [[CrossRef](#)]
10. Ho, W.; Yu, J.C.; Lin, J.; Yu, J.; Li, P. Preparation and Photocatalytic Behavior of Li MoS₂ and WS₂ Nanocluster Sensitized TiO₂. *Langmuir* **2004**, *14*, 5865–5869. [[CrossRef](#)]
11. Splendiani, A.; Sun, L.; Zhang, Y.; Li, T.; Kim, J.; Chim, C.Y.; Galli, G.; Wang, F. Emerging Photoluminescence in Monolayer MoS₂. *Nano Lett.* **2010**, *4*, 1271–1275. [[CrossRef](#)]
12. Eda, G.; Yamaguchi, H.; Voiry, D.; Fujita, T.; Chen, M.; Chhowalla, M. Photoluminescence from Chemically Exfoliated MoS₂. *Nano Lett.* **2011**, *12*, 5111–5116. [[CrossRef](#)] [[PubMed](#)]
13. Coleman, J.N.; Lotya, M.; O'Neill, A.; Bergin, S.D.; King, P.J.; Khan, U.; Young, K.; Gaucher, A.; De, S.; Smith, R.J.; et al. Two-Dimensional Nanosheets Produced by Liquid Exfoliation of Layered Materials. *Science* **2011**, *6017*, 568–571. [[CrossRef](#)] [[PubMed](#)]

14. Štengl, V.; Henych, J. Strongly Luminescent Monolayered MoS₂ Prepared by Effective Ultrasound Exfoliation. *Nanoscale* **2013**, *8*, 3387–3394. [[CrossRef](#)]
15. Lin, T.W.; Dhenadhayalan, N.; Lee, H.L.; Lin, Y.T.; Lin, K.C.; Chang, A.H. Fluorescence Turn-on Chemosensors Based on Surface-Functionalized MoS₂ Quantum Dots. *Sens. Actuators B Chem.* **2019**, *281*, 659–669. [[CrossRef](#)]
16. Wu, Q.; Wang, X.; Jiang, Y.; Sun, W.; Wang, C.; Yang, M.; Zhang, C. MoS₂-Qd-Based Dual-Model Photoluminescence Sensing Platform for Effective Determination of Al³⁺ and Fe³⁺ Simultaneously in Various Environment. *ChemistrySelect* **2018**, *8*, 2326–2331. [[CrossRef](#)]
17. Roy, S.; Bobde, Y.; Ghosh, B.; Chakraborty, C. Targeted Bioimaging of Cancer Cells Using Free Folic Acid-Sensitive Molybdenum Disulfide Quantum Dots through Fluorescence “Turn-Off”. *ACS Appl. Bio Mater.* **2021**, *3*, 2839–2849. [[CrossRef](#)]
18. Ji, Q.; Zhang, Y.; Gao, T.; Zhang, Y.; Ma, D.; Liu, M.; Chen, Y.; Qiao, X.; Tan, P.; Kan, M.; et al. Epitaxial Monolayer MoS₂ on Mica with Novel Photoluminescence. *Nano Lett.* **2013**, *8*, 3870–3877. [[CrossRef](#)]
19. Lu, X.; Utama, M.I.B.; Lin, J.; Gong, X.; Zhang, J.; Zhao, Y.; Pantelides, S.T.; Wang, J.; Dong, Z.; Liu, Z.; et al. Large-Area Synthesis of Monolayer and Few-Layer MoSe₂ Films on SiO₂ Substrates. *Nano Lett.* **2014**, *5*, 2419–2425. [[CrossRef](#)]
20. Haldar, D.; Dinda, D.; Saha, S.K. High Selectivity in Water Soluble MoS₂ Quantum Dots for Sensing Nitro Explosives. *J. Mater. Chem. C* **2016**, *26*, 6321–6326. [[CrossRef](#)]
21. Hakey, P.; Ouellette, W.; Zubieta, J.; Korter, T. Redetermination of Cyclo-Trimethylenetrinitramine. *Acta Crystallogr. Sect. E* **2008**, *8*, o1428. [[CrossRef](#)] [[PubMed](#)]
22. Wyman, J.F.; Serve, M.P.; Hobson, D.W.; Lee, L.H.; Uddin, D.E. Acute Toxicity, Distribution, and Metabolism of 2,4,6-Trinitrophenol (Picric Acid) in Fischer 344 Rats. *J. Toxicol. Environ. Health* **1992**, *2*, 313–327. [[CrossRef](#)]
23. Chakraborty, I.; Pradeep, T. Atomically Precise Clusters of Noble Metals: Emerging Link between Atoms and Nanoparticles. *Chem. Rev.* **2017**, *12*, 8208–8271. [[CrossRef](#)]
24. Zhang, X.; Zhang, G.; Wei, G.; Su, Z. One-Pot, In-Situ Synthesis of 8-Armed Poly(Ethylene Glycol)-Coated Ag Nanoclusters as a Fluorescent Sensor for Selective Detection of Cu²⁺. *Biosensors* **2020**, *10*, 131. [[CrossRef](#)]
25. Zhang, Z.; Loebus, A.; de Vicente, G.; Ren, F.; Arafeh, M.; Ouyang, Z.; Lensen, M.C. Synthesis of Poly(Ethylene Glycol)-Based Hydrogels Via Amine-Michael Type Addition with Tunable Stiffness and Postgelation Chemical Functionality. *Chem. Mater.* **2014**, *12*, 3624–3630. [[CrossRef](#)]
26. Ren, F.; Yesildag, C.; Zhang, Z.; Lensen, M.C. Functional Peg-Hydrogels Convey Gold Nanoparticles from Silicon and Aid Cell Adhesion onto the Nanocomposites. *Chem. Mater.* **2017**, *5*, 2008–2015. [[CrossRef](#)]
27. Wang, Y.; Ni, Y. Molybdenum Disulfide Quantum Dots as a Photoluminescence Sensing Platform for 2,4,6-Trinitrophenol Detection. *Anal. Chem.* **2014**, *15*, 7463–7470. [[CrossRef](#)] [[PubMed](#)]
28. Xu, S.; Lu, H. Mesoporous structured MIPs@CDs fluorescence sensor for highly sensitive detection of TNT. *Biosens. Bioelectron.* **2016**, *15*, 7463–7470. [[CrossRef](#)] [[PubMed](#)]
29. Xu, S.; Lu, H. Ratiometric fluorescence and mesoporous structure dual signal amplification for sensitive and selective detection of TNT based on MIP@QD fluorescence sensors. *Chem. Commun.* **2015**, *51*, 3200–3203. [[CrossRef](#)]